2004

A Uniform Property Region Method for Screw Compressor's End-Face Leakage Prediction

Calim Zamfirescu
Delft University of Technology

Carlos A. Infante Ferreira
Delft University of Technology

A UNIFORM PROPERTY REGION METHOD FOR SCREW COMPRESSORS' END-FACE LEAKAGE PREDICTION

C. ZAMFIRESCU, C. A. INFANTE FERREIRA

Delft University of Technology, Section Engineering Thermodynamics
Mekelweg 2, 2628 CD Delft, The Netherlands, fax: +31.15.2782460

ABSTRACT

Based on the assumption of a uniform property annular-shaped region at the labyrinth entrance, this paper proposes a method for leakage flow rate prediction at the discharge end-face of twin-screw compressors. Assumption of such a region is the key aspect in the construction of an equivalent network of end-face leakage flows, in which the labyrinth entrance zone is a node. Using mass and energy conservation laws, the thermo-physical properties of the *average-state region (ASR)*, and leakage paths flow rates are determined. The method is validated against experimental data obtained on an oil-free twin-screw compressor working with an ammonia-water mixture. The method allows for identification of additional leakages into cavities that are at the beginning of the compression process. Consequently it improves the accuracy of previous models.

1. INTRODUCTION

Due to their incontestable advantages (high pressure ratios, high compactness, small number of moving parts, low maintenance requirements, etc.), twin-screw compressors showed in the last decades to be attractive solutions for multiple applications. The estimation of leakage flows remains one of the most important problems related to screw compressor design, performance prediction, and know-how.

When dealing with high pressure oil-free applications, as for example in the field of refrigeration and heat pumps – see Itard (1998) – it is highly desirable to possess an accurate method for leakage estimation, while the refrigerant that eventually leaks out of the compressor housing must be collected and re-injected into the compression process. The working fluid leaks out through the labyrinth seal that must be mounted on the shaft at the discharge side of oil-free screw compressors in order to prevent a too high wear rate of the lip seals.

On the other hand, the screw compressor performance is highly affected by the internal leakages. Fleming and Tang (1995) identified up to six different types of leakage paths in twin-screw compressors.

Among several kinds of particular leakage paths studied by different authors – You (1994), Singh and Bowman (1990), Zaytsev (2003), the leakages that take place at the rotors' discharge end-face clearance are probably the most difficult to predict. At the end-face, the leakage flows driven by spatially and time dependant pressure differences, have a very complicated pattern.

Figure 1 (a) presents the discharge end-face of a screw compressor having a $z_1=5$ lobes male rotor. One important leakage path – illustrated with white arrows – is formed between any leading cavity and the corresponding trailing cavity. The pressures of leading and trailing cavities have a phase shift of $\Delta j = 2p/z_1$. Zaytsev (2003) investigated this kind of leakage by using an isentropic expansion model in order to estimate the fluid velocity. He assumed that the leakage path length is equal with the male plus female lobe height (i.e. segments of type A_1A_2, B_1B_2, C_1C_2, and D_1D_2 etc.). He also assumed that the leakage path length decreases linearly down to zero when the male and female rotors' lobes come into contact. Furthermore, while the cavity in the suction phase opens to the end-face during the compressor's cycle, leakages through the end-face clearance towards suction were also considered.

In this paper two other possible leakage flows are investigated that superimpose to the above discussed leakages at the end-face: (i) the flow between cavities being at a higher phase of the compression process towards the cavities that are at the beginning of the compression process (see Figure 1 (a) – black arrows), and (ii) the flow through the

labyrinth seal (see Figure 1 (b) – black arrows). A prediction method for the leakage flow rates (i) and (ii) is also proposed.

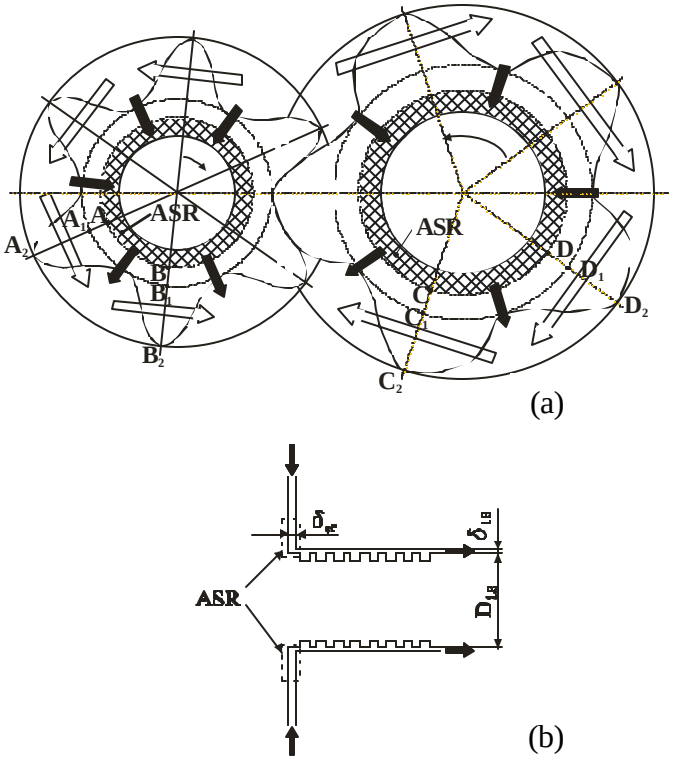

Figure 1 Flow leakage paths at the discharge end-face, and the *ASR* around the labyrinth

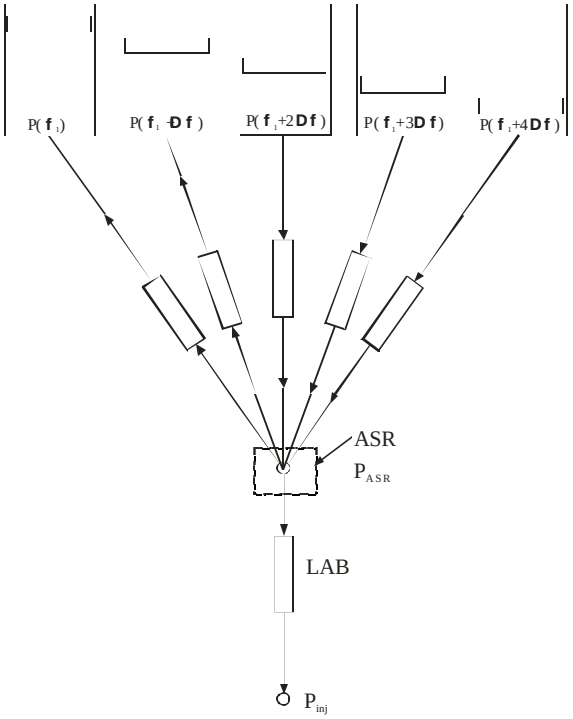

Figure 2 Leakage model for the discharge end-face of screw compressors

2. PROPOSED METHOD FOR LEAKAGE PREDICTION

Assume that in an annular region around the labyrinth entrance – as indicated with the notation *ASR* (*Average-State Region*) on Figure 1 (a) and (b) – the working fluid has uniform thermodynamic properties. This assumption is reasonable if it is considered that the fluid at the entrance of the labyrinth clearance (close to the shaft perimeter) is well mixed due to the movement of the rotors.

This allows for the construction of an equivalent network of leakage paths, as it is presented in Figure 2. The cavities being at a more advanced compression phase deliver fluid to the *ASR*. By contrary, the cavities being at the beginning of the compression process, receive fluid from the *ASR*, while they have a lower pressure. The flow also leaks from the *ASR* through the labyrinth clearance and it is eventually re-injected into the process at a lower pressure, P_{inj}. Note that the leakage flows from leading to trailing cavities are not represented in the network of Figure 2. These leakages are treated separately and superimposed to the ones derived with the *ASR* model.

In order to evaluate the leakage flows, two questions have to be clarified: (i) what is the velocity of each flow, and (ii) what is the leakage area normal to the flow.

The simplest flow model widely used in simulation of screw compressors is the converging nozzle flow model, with assumptions that the compressible flow is isentropic and the pressure in the narrowest part of the flow path is equal to the downstream cavity pressure – see Fujiwara *et al*. (1974), Sauls (1996). The model is based on the balance of inertia and pressure forces, while viscous forces are neglected. The flow velocity obtained with this model is

$$W(j_1)=\left[\sqrt{2\int_{P_{down}}^{P_{up}} v\,dP}\right]_{j_1} \tag{1}$$

Zaytsev (2003) proved the acceptable applicability of equation (1) even for azeotropic refrigerants (as ammonia-water solutions) where the non-isothermal phase change process complicates the mathematical treatment, and the viscous effect should not be neglected. Note that the flow velocity is bounded by the local speed of sound.

The calculated flow rate based on the velocity given by equation (1) is adjusted by an empirical flow coefficient, C_0.

$$\dot{m}(j_1)=C_0\left[rA_{ef}W\right]_{j_1} \tag{2}$$

The flow coefficient is usually found from experiments – Prins and Infante Ferreira (2000), or from comparisons with more elaborated models – Fujiwara and Osada (1995), Zaytsev and Infante Ferreira, (2000).

With reference to Figure 1 (a) the end-face leakage area between any cavity and *ASR* it was assumed to be given by

$$A_{ef}(j_1)=\left[l_{AB}+l_{CD}\right]_{j_1}d_{ef} \tag{3}$$

where l_{AB} and l_{CD} have maximal values (see Figure 1) when both tips of the lobes that form the cavity are directed to the housing. This situation stands for almost all compression and discharge phases, except for the short period when the male and female lobes contact each other. In that period the leakage area between the cavity and *ASR* goes down to zero; this reduction was assumed linear, as it is represented in Figure 3 in a dimensionless format. For the computations performed in this paper the position of the arcs *AB* and *CD* is considered at an average radius between those corresponding to labyrinth and rotors' base circles.

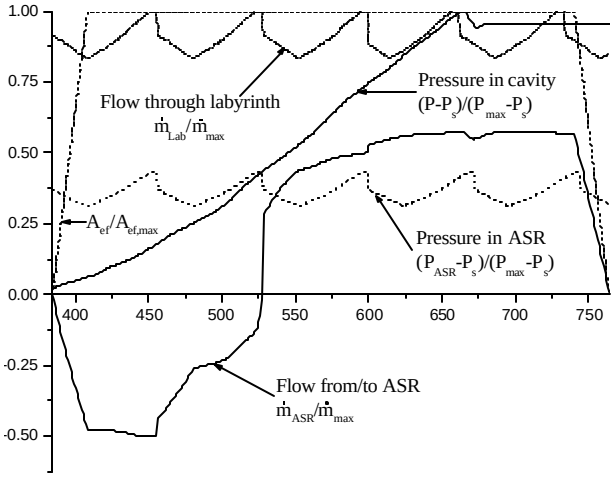

Figure 3 Leakages at the end-face and related parameters in experimental conditions A

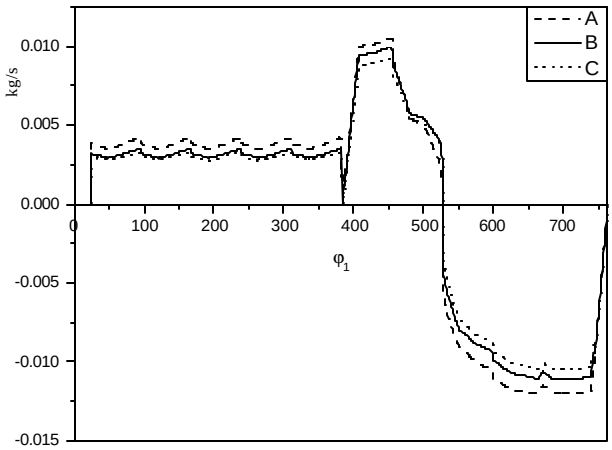

Figure 4 Leakages in or out for a working cavity, estimated in three experimental conditions

The mass conservation in *ASR*, based on the leakage network from Figure 2, is

$$\dot{m}_{Lab}(j_1)=\sum_{i=1}^{z_1}\dot{m}_{\left(j_1+(i-1)\frac{2p}{z_1}\right)} \tag{4}$$

The LHS term in equation (4) refers to the mass flow rate that leaks through the labyrinth seal. The prediction of leakage mass flow rate in labyrinths has been extensively studied in the field of turbomachinery and compressor engineering – Childs (1984), Yucel and Kazakia (2001). The analytical prediction technique of Yucel and Kazakia (2001), which considers that the leakage flow rate through the labyrinth depends on the downstream/upstream pressure ratio and the geometrical characteristics of the labyrinth, has been adapted:

$$\dot{m}_{Lab}(j_1)=C_0F_{Lab}\frac{P_{ASR}}{(Pv)^{1/2}}\left[1-\left(\frac{P_{inj}}{P_{ASR}}\right)^2\right]^{1/2} \tag{5}$$

where P_{inj} represents the pressure at the injection port, where the fluid that leaks through the labyrinth is re-injected into the compression process.

The geometrical factor F_{Lab} depends on the annular passage area of the labyrinth, and the number of labyrinth teeth

$$F_{Lab} = A_{Lab} \Big/ \left[1 + (N-1)\Big/(1 + 0.0791(N-1))^2\right]^{1/2} \tag{6}$$

In the case of twin screw compressors there are two rotors – male and female, and both have labyrinths mounted on the shaft. The passage area is

$$A_{Lab} = p\left(D_1 d_1 + D_2 d_2\right) \tag{7}$$

The average value $\overline{(Pv)}$ used in equation (5) is calculated from:

$$\overline{(Pv)}_{j_1} = \left[(Pv)_{ASR,j_1} + (Pv)_{inj}\right]\Big/2 \tag{8}$$

Yucel and Kazakia (2001) considered, as the majority of the studies found in literature do, that the flow through labyrinths is isothermal and obey the ideal gas law. They used RT in the equation, instead of $\overline{(Pv)}$. By replacing RT with an average value of $\overline{(Pv)}$ in our study, the applicability of the model is extended to real fluids. Furthermore it is assumed that the flow coefficient C_0 has the same value for both labyrinth flow and end-face leakage flows. In both cases, C_0 takes the entropy production during the expansion process into account.

Substitution of equations (2) and (5) into the mass conservation equation (4) leads to

$$F_{Lab}\left\{\frac{P_{ASR}}{\overline{(Pv)}^{1/2}}\left[1-\left(\frac{P_{inj}}{P_{ASR}}\right)^2\right]^{1/2}\right\}_{j_1} = \sum_{i=1}^{z_1}\left(r A_{ef} W\right)_{j_1+(i-1)\frac{2p}{z_1}} \tag{9}$$

Assuming that P_{inj} and the thermodynamic state at all compression cavities $(i=1..z_1)$ are known, the only unknown in equation (9) remains the thermodynamic state of *ASR*. This is defined by two parameters: the temperature, T_{ASR} and the pressure, P_{ASR}. A second equation is then needed in order to determine the thermodynamic state of *ASR*. This equation comes from the energy conservation law of all z_1 leakage flows that enter or leave the *ASR* at the end-face of the screw compressor rotors.

The flow velocity through the end-face clearance is high, and since the flow is compressible, it can reach the speed of sound. The flow has no time to undergo a significant heat exchange with the rotors and housing. In this case, the conservation of energy of each of the z_1 flows is written as

$$h_{ASR}(j_1) + 0.5W_{ASR}^2\left(j_1+(i-1)\frac{2p}{z_1}\right) = \left(h + 0.5W^2\right)\left(j_1+(i-1)\frac{2p}{z_1}\right), \quad i = 1..z_1 \tag{10}$$

where W_{ASR} is the flow velocity at the *ASR* boundary, while W is the flow velocity at the working cavity boundary. These velocities are expressed in function of the mass flow rate, flow passage area, and the specific volume

$$W_{ASR}(j_1) = \left(\dot{m}\Big/A_{ef}\right)\left(j_1+(i-1)\frac{2p}{z_1}\right) v_{ASR}(j_1), \quad i = 1..z_1 \tag{11}$$

$$W(j_1) = \left[\dot{m}v\Big/A_{ef}\right]_{(j_1)} \tag{12}$$

Multiplying all the z_1 energy conservation equations (11) with $\dot{m}_{\left(j_1+(i-1)\frac{2p}{z_1}\right)}$ and adding them, we obtain

$$F_{Lab}\left[\frac{P_{ASR}}{\overline{(Pv)}^{1/2}}\left[1-\left(\frac{P_{inj}}{P_{ASR}}\right)^2\right]^{1/2} h_{ASR}\right]_{j_1} = \sum_{i=1}^{z_1}\left\{r A_{ef} W\left[h + 0.5\left(W^2 - W_{ASR}^2\right)\right]\right\}_{j_1+(i-1)\frac{2p}{z_1}} \tag{13}$$

The fluid enthalpy in *ASR*, h_{ASR} is linked through the equation of state to fluid's temperature, T_{ASR} and pressure, P_{ASR}. In the general case of mixtures, the enthalpy depends also on concentration species. For a two-component homogeneous mixture with overall concentration X_o

$$h_{ASR} = h\left(P_{ASR}, T_{ASR}, X_o\right) \tag{14}$$

A simple Newton-Rapson method can be used to solve the system of equations (9) and (13) for P_{ASR} and T_{ASR}. The initial value of P_{ASR} can be set as the average of discharge and injection pressure, while the initial guess of temperature can be chosen as the average value of the temperatures in the different cavities.

Knowing the leakage mass flow rates is not enough for completing a thermodynamic model of the compressor. It is necessary to know simultaneously the thermodynamic parameters with which the leakage flows leave or enter the working cavity. The enthalpy of flows that leave the working cavities is supposed known, while the cavity working pressure and temperature are known. The flows that leave the *ASR* have the specific entropy

$$s_{ASR} = s(P_{ASR}, T_{ASR}, X_o) \tag{15}$$

and when they enter in another cavity at current pressure *P*, considering an isentropic expansion, they will enter with enthalpy h_{in}:

$$h_{in} = h(P, s_{ASR}, X_o) \tag{16}$$

3. EXPERIMENTAL VALIDATION

The proposed method has been validated with experimental results obtained by Zaytsev (2003) with an oil-free screw compressor operating under wet conditions with ammonia-water as working fluid. Three sets of experimental results are available, as presented in *Table 1*. Furthermore, the experimentally determined *PV* diagrams were available in all three cases.

Figure 3 presents the cavity pressure during the compression and discharge phases for experimental conditions *A*. The pressure is plotted in a dimensionless format, as indicated on the figure, against the male rotor angle j_1. The suction phase takes place for $j_1 = 24...384^o$, the compression phase for $j_1 = 384...658^o$, and the discharge phase for $j_1 = 658...764^o$.

Table 1 Experimental Results

Experimental Condition	A	B	C
Suction pressure, bar(a)	3.70	3.28	3.09
Discharge pressure, bar(a)	9.08	8.08	7.58
Suction temperature, °C	62.8	62.6	62.4
Discharge temperature, °C	98.2	95.5	95.3
Mixture concentration, kg/kg	0.376	0.364	0.351

The system of equations (9) and (13) has been solved as a function of the rotation angle j_1 in the compression-discharge range, using parameters applicable for the conditions of the experiments.

The results are reported in a non-dimensional form in Figure 3 so that the correspondence with the operating conditions can be visualized. In the beginning of compression, the pressure of *ASR* is higher than the pressure of the current cavity, as can be observed on the plot. The *ASR* pressure varies periodically with a period of $2p/z_1 = 72^o$.

As the end-face leakage path area starts to grow from 0 to 100%, a leakage from *ASR* toward to the cavity initiates. The leakage reaches its maximum at the end of first compression phase, i.e *456°*. In the second compression phase the leakage to the cavity decreases down to zero, while the cavity's pressure increases, and reaches the *ASR* pressure at the end of second compression phase, i.e. *528°*.

During the rest of compression and discharge process the cavity pressure is higher than that of the *ASR*, and consequently, a leakage initiates from the cavity, towards the *ASR*. This leakage decreases to zero in the last part of the compressor's cycle, when the end-face leakage area (A_{ef}) goes down to zero, too. The flow that leaks through the labyrinth during compression and discharge process has an oscillation period of $2p/z_1$. The cavities that are at a higher phase of compression, or in discharge process, have a pressure that is higher than that of the *ASR*. These cavities deliver a leakage flow to the *ASR*. From there the flow is directed through the end-face clearance towards the cavities being in an initial phase of compression since they have a pressure lower than that of the *ASR*. A leakage exists also through the labyrinth towards the cavity where the working fluid is re-injected into the process. That cavity has the pressure P_{inj}.

In all the experiments shown in *Table 1*, the labyrinth leakage flow was re-injected into the suction, so that $P_{inj} = P_s$. During the suction phase, there are always z_1 cavities connected to the suction port. This means that the flow received from the labyrinth by each cavity can be approximated with $\dot{m}_{Lab} / z_1$.

The flow from the ASR that enters or leaves a working cavity is, for all three experimental situations, *A*, *B*, and *C*, presented in Figure 4. During the suction phase, the flow leaking from the *ASR* through the labyrinth is delivered to the corresponding cavity. During the first two compression phases – $j_1 = 384...528^o$ a leakage flow coming from the *ASR* enters the cavity through the end-face clearance. During the last part of compression and discharge phase – $j_1 = 528...764^o$ a flow leaks from the cavity and enters the *ASR*, from where it is distributed through the end-face clearance to the cavities being at the beginning of the compression process, and through the labyrinth clearance to the cavities being in suction phase.

The three plots in Figure 4 show a similar trend, the only difference being the magnitude of the flow, which corresponds to the magnitude of the discharge pressure.

A comparison between predicted and measured *PV* diagram is presented in Figure 5 for experimental case *C*. The *PV* diagram was predicted based on the compressor's model developed by Zaytsev (2003). The labyrinth flow in Zaytsev's model is assumed constant and proportional with the difference between discharge and suction pressure. All the flow leaking through the labyrinth was re-injected into the suction port.

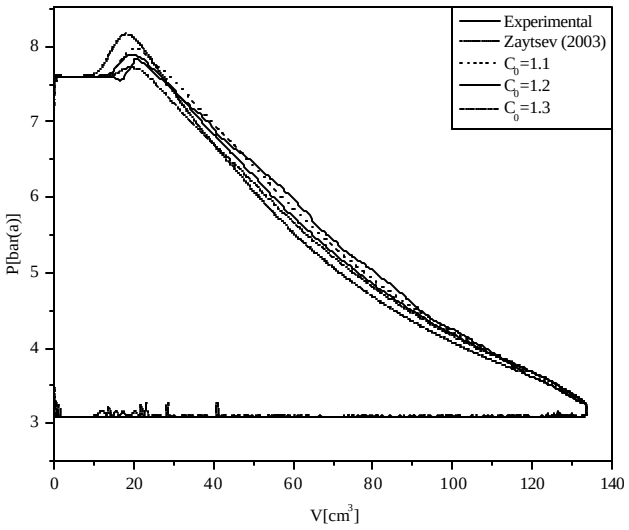

Figure 5 Computed vs measured PV diagram for experimental conditions C

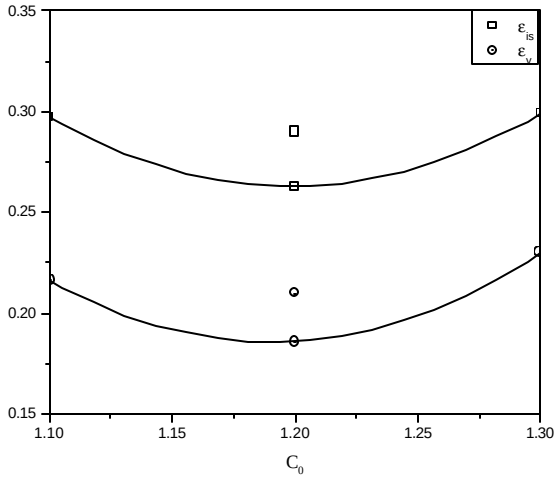

Figure 6 The sensitivity of the flow coefficient C_0

Zaytsev's model results for a C_0 flow coefficient of *1.2* are also shown in Figure 5. It can be observed that at the beginning of compression, the measured pressure in the compressor's cavity increases faster than predicted.

Zaytsev's model has been modified to include the additional leakages from the *ASR*. The results are presented in the same plot for three values of the flow coefficient C_0. In these simulations, the dynamic linked library developed by Zamfirescu (2001) was used for the ammonia-water property computations. The library is based on Ziegler and Trepp (1984) equations for ammonia-water properties.

The results validate the *ASR* method for leakage prediction at the end-face. The additional leakages that flow into the cavities at the beginning of the compression process, predicted by *ASR* model, induce a rapid growth of cavity pressure. This is much closer to the experimental evidence, than the original predictions by Zaytsev (2003).

For the same C_0 coefficient of *1.2* used by Zaytsev, the new model prediction fits better the experimental *PV* diagram. Increasing C_0 means larger leakages through the labyrinth and consequently lower pressures in the

compression cycle (see curve for $C_0=1.3$). A reduced flow coefficient means less labyrinth leakage, and this induces higher pressure values during the compression cycle. The pressure curve corresponding to $C_0=1.1$ fits very well the measurements, even though the predicted peak discharge pressure is higher than the measured one.

In order to compare the predicted results with the experimental determinations some other indicators should be considered together with the *PV* diagram. They have to include the discharge mass flow rate and the compressor's power (i.e. work). The definition of isentropic efficiency introduced by equation (17) indicates that it is a measure of both discharge mass of refrigerant and compressor's work per cycle.

$$h_{is} = (h_{is} - h_s) M_{disch} / w \tag{17}$$

The volumetric efficiency – equation (18) – is a true measure of the discharge mass flow rate.

$$h_V = M_{disch} v_s / V_{\max} \tag{18}$$

By using the mean square root error defined by equation (19) both efficiencies have been compared with the measurements.

$$e = \left\{ \left[(h - h_{ex}) / h_{ex} \right]_A^2 + \left[(h - h_{ex}) / h_{ex} \right]_B^2 + \left[(h - h_{ex}) / h_{ex} \right]_C^2 \right\}^{0.5} \tag{19}$$

The results are displayed in Figure 6 for both isentropic efficiency prediction error – e_{is}, and volumetric efficiency error – e_V. The plot was drawn for flow coefficients of *1.1*, *1.2*, and *1.3*. The curves are polynomial fits to the results. Figure 6 shows also the results of Zaytsev (2003), that are available only for $C_0=1.2$.

In terms of mean square root error e_V, the improvement brought by the *ASR* model in prediction of volumetric efficiency is in the order of 4 – 5%. A better prediction of volumetric efficiency means a better prediction of the discharge mass flow rate – see equation (18). On the other hand, the evidently better prediction of the experimental *PV* diagram obtained with *ASR* model, not only proves the existence of additional leakages during the beginning of the compression process, but in the same time assures a better prediction of the compressor's work. According to equation (17) an improved prediction of both the work and discharge mass flow rate induces an increased accuracy of the model in isentropic efficiency estimation. Results on Figure 6 show that the prediction improvement for isentropic efficiency is in the same order of that of volumetric efficiency.

4. CONCLUSIONS

In conclusion, for prediction of twin screw compressors end-face leakage it is useful to assume an *average-state region* around the labyrinth entrance (or at the shaft base if a labyrinth seal is not present). The assumption of an *ASR* facilitates the construction of a network representing the discharge end-face leakages (Figure 2).

The obtained results demonstrate the existence of important leakages into the cavities at the initial stage of compression process. These leakage flows enter the cavities directly from the *average-state region*. They originate from the cavities that are at a more advanced stage of compression, or in the discharge phase.

Optimal values – i.e. best fitted to the experiments – of the flow coefficient C_0 fall in a close range around *1.2*. As it was presented in section 2, the flow coefficient takes into account the difference between the real leakage flow rate and the one predicted by the isentropic expansion model. Several authors showed that the flow coefficient is lower than unity – that is the real mass flow rate should be lower than that predicted with the isentropic expansion model. In the analysis made by Zaytsev (2003), he showed theoretically that the expected flow coefficient for expansion of ammonia-water solution should fall in the range of 0.5 to 0.7. As shown in this paper, the C_0 value is approximately *1.2*. This coefficient clearly includes a correction to the estimated leakage flow passage area (equation (2)).

It is very difficult to estimate accurately all the real clearances for a particular compressor. The compressor model discussed here considers 7 different leakage paths including the labyrinth. The presence of a non-linear thermal expansion of rotors and housing, together with a difficult-to-predict running tolerances, makes the accurate estimation of leakage paths areas a very difficult task.

NOMENCLATURE

A	flow passage area, m^2
C_0	flow coefficient
D	shaft diameter, m
F	labyrinth factor, eq. (6), m^2
h	enthalpy, J/kg
l	leakage path length, m
M	mass, kg
$\dot{m}$	mass flow rate, kg/s
N	number of labyrinth teeth
P	pressure, Pa
R	gas constant, J/kgK
s	specific entropy, J/kgK
T	temperature, K
v	specific volume, m^3/kg
V	volume, m^3
W	fluid velocity, m/s
w	work, J
X	concentration, kg/kg
z	number of rotor lobes

Greek letters

e	estimation error
h	efficiency
r	density, kg/m^3
j	rotation angle, deg

Subscripts

1	male rotor
2	female rotor
A,B,C	experimental run index
ASR	average-state region
$disch$	discharge
ef	end-face
ex	experimental
i	index
in	intake
inj	injection
is	isentropic
Lab	labyrinth
max	maximum value
s	suction
o	overall
V	volumetric

Superscripts

$\overline{(\ )}$	averaged value

REFERENCES

Childs, D., 1984, Turbomachinery rotordynamics phenomena, modeling, and analysis. John Wiley and Sons, New York, pp. 290-354

Fleming, J.S., and Tang, Y., 1995, The analysis of leakage in a twin screw compressor and its application to performance improvement. IMechE Journal of Process Mechanical Engineering, Proc. Instn. Mech. Engrs. Vol. 209, pp125-136

Fujiwara M., Mori, H., Suwama, T., 1974, Prediction of the oil-free compressor performance using digital computer. Proceedings Purdue Compressor Technology Conference, West Lafayette, Indiana, pp. 186-189

Fujiwara, M. and Osada, Y., 1995, Performance analysis of oil injected screw compressors and its applications. International Journal of Refrigeration, vol. 18(4), pp. 220-227

Itard, L., 1998, Wet compression-resorption heat pump cycles: thermodynamic analysis and design. Ph.D. Thesis, Delft University of Technology, The Netherlands

Prins, J., and Infante Ferreira, C.A., 2000, Feasibility and design of leakage experiments on a running twin screw compressor. In: 'From Thermo-Economics to Sustainability' Eds. Hirs, G., Part 2: ECOS 2000 Proceedings, University of Twente, Netherlands, pp.869-880

Sauls, J., 1996, Development of a comprehensive thermodynamic modeling system for refrigerant screw compressors. Proceedings Purdue Compressor Technology Conference, West Lafayette, IN, vol. 1, pp. 151-156

Singh, P.J., and Bowman, J.L., 1990, Calculation of the blow hole area for screw compressors. Proceedings of the 1990 International Compressor Engineering Conference, Purdue University, Purdue, Indiana, vol. 2, pp. 938-948

You, C.X., 1994, A theoretical study of rotor forces and torques in helical twin screw compressors. Ph.D. Thesis, University of Strathclyde, Glasgow

Yucel, U., and Kazakia, J., 2001, Analytical prediction techniques for axisymetric flow in gas labyrinth seals. Journal of Engineering for Gas Turbines and Power, v.123, pp. 255-257

Zamfirescu, C., 2001, Dynamic link library for ammonia-water thermophysical properties computation. Report K302, Delft University of Technology

Zaytsev, D., 2003, Development of wet compressor for applications in compression-resorption heat pumps, Ph. D. Thesis, Delft University of Technology, The Netherlands

Zaytsev, D., and Infante Ferreira, C.A., 2000, Aspects of two-phase flow screw compressor modeling – Part I: Leakage flow and rotor tip friction. Proceedings International Compressor Engineering Conference, Purdue, West Lafayette, Indiana, vol. 2, pp. 893-899

Ziegler, B., and Trepp, Ch., 1984, Equation of state for ammonia-water mixture. International Journal of Refrigeration, vol. 7(2) pp. 101-106

ACKNOWLEDGEMENTS

This work has been funded in part by NOVEM, grant BSE – NEO 0268.02.02.03.0002. The authors further acknowledge Dr. Zaytsev for his advices during the implementation of the *ASR* model.